Supporting Information

Fundamental Insights into the Reductive Covalent Cross-Linking of Single-Walled Carbon Nanotubes

Milan Schirowski[a,b],§, Gonzalo Abellán[a,b],§, Edurne Nuin[a], Jonas Pampel[c], Christian Dolle[d], Vincent Wedler[b], Tim-Patrick Fellinger[e,f], Erdmann Spiecker[d], Frank Hauke[b], and Andreas Hirsch*[a,b]

[a] M. Schirowski, Dr. G. Abellán, Dr. E. Nuin, Dr. F. Hauke, Prof. Dr. A. Hirsch
Chair of Organic Chemistry II
Friedrich-Alexander-Universität Erlangen-Nürnberg
Henkestr. 42, 91054 Erlangen, Germany

* andreas.hirsch@fau.de

§ These authors contributed equally to this work.

[b] M. Schirowski, Dr. G. Abellán, V. Wedler, Dr. F. Hauke, Prof. Dr. A. Hirsch
Joint Institute of Advanced Materials and Processes
Friedrich-Alexander-Universität Erlangen-Nürnberg
Dr.-Mack-Str. 81, 90762 Fürth, Germany

[c] Dr. J. Pampel
Fraunhofer Institute IWS
Winterbergstr. 28, 01277 Dresden, Germany

[d] C. Dolle, Prof. E. Spiecker
Institute of Micro- and Nanostructure Research
Friedrich-Alexander-Universität Erlangen-Nürnberg
Cauerstrasse 6, 91058 Erlangen, Germany

[e] Dr. T.P. Fellinger
University of *Applied Science Zittau/Görlitz*
Theodor-Körner Allee 16, 02763 Zittau, Germany

[f] Dr. T.P. Fellinger
Department of Technical Electrochemistry, Technical University Munich
Lichtenbergst*raße 4, 85748 Garching, Germany*

1 Additional Experimental Information

Materials:

HiPco SWCNTs (diameter 0.8 – 1.2 nm, length 100 – 1,000 nm) were purchased by Unidym (batch #P2772). Chemicals were purchased from Aldrich and Acros Organics and were used as received. 1,5-diiodonaphthalene, 4,4''-diiodo-*p*-terphenyl and 4,4'''-diiodo-1,1':4',1'':4'',1'''-quaterphenyl were synthesized according to reported literature procedures.[1]

Information about the SWCNT used in this study:

Elicarb (batch 121212/31): Diameter: 0.9 – 1.7 nm; length: 1,000 nm; iron content: 1 %; BET area: 700 m^2/g

HiPco (Unidym, batch # P2772): Diameter: 0.8 – 1.2 nm; iron content: 15 %; length: 100 – 1,000 nm; BET area: 400 – 1,000 m^2/g

Synthesis of BDS:

15 mmol of the corresponding diamine (p-phenylenediamine or benzidine) was dispersed in 120 mL of water. Then, 12 mL HBF_4 solution (47 %) was added forming a neat solution. The solution was cooled by an ice bath and 55 mmol of saturated $NaNO_2$ solution was added dropwise via a dropping funnel, not exceeding 5 °C. After complete addition, the formed precipitate was collected, filtered, and washed with 20 mL of ice-cold water and 50 mL diethyl ether. After finally drying in vacuo for 24 h, the BDS (benzene-1,4-bisdiazonium tetrafluoroborate or biphenyl-4,4'-bisdiazonium tetrafluoroborate) was yielded (86 %).

Purifying of DMAc and THF:

The HPLC-grade solvent were dried over molecular sieve (3 Å, 15 %/w) for 3 days and the remaining water content of <10 ppm determined by Karl-Fischer titration. Subsequently, the solvent was deoxygenated by the freeze-pump-thaw degassing procedure (4 cycles).

Glovebox:

Sample functionalization was carried out in an argon-filled Labmaster$_{pro}$ sp glovebox (MBraun), equipped with a gas purifier and solvent vapor removal unit, with an oxygen content <0.1 ppm and a water content <0.1 ppm.

Raman spectroscopy:

Measurements were performed on a LabRam Aramis system. Maps of 100 µm x 100 µm were recorded with a step size of 4 µm, yielding a total of 676 single-point spectra with acquisition times of 0.2–1.0 s, depending on the quality of the spectrum. Laser excitation wavelengths were 532 nm and 785 nm, laser power was <1 W to avoid defunctionalization.

Temperature-dependent Raman spectroscopy:

Temperature-dependent Raman measurements were performed in a Linkam stage THMS 600, equipped with a liquid nitrogen pump TMS94 for temperature stabilization under a constant flow of nitrogen. The measurements were carried out on Si/SiO_2 substrates (300 nm oxide layer) with a heating rate of 10 $K \cdot min^{-1}$.

Thermogravimetric analysis (TGA) combined with gas-chromatographic separation (GC) and coupled with a mass spectrometer (MS)

Thermogravimetric analysis was carried out on a PerkinElmer Pyris 1 TGA instrument. Time-dependent temperature profiles in the range of 20 and 700 °C (20 $K\,min^{-1}$ gradient) were recorded under a constant flow of N_2 (70 $mL\,min^{-1}$).[5] About 2.0 mg initial sample mass were used. The evolved gases detached from the respective sample in combination with the N_2 carrier gas is transferred into the GC system through a TL9000 TG-IR-GC interface at a constant temperature of 280 °C. The gas-chromatographic separation was achieved by a GC-Clarus 680 with a polysiloxane-coated Elite-5MS capillary column: 30 m length, 0.25 mm diameter, 0.25 µm film thickness. A GC injection fraction of 150 µL was collected at the selected TG temperature (in the range of 200–300 °C), parameters: injector zone = 280 °C, detection zone = 250 °C, flow rate helium = 10 $mL\,min^{-1}$, temperature profile = 34 min total run time, dynamic ramp = 24 min, 40–280 °C with a 10 $K\,min^{-1}$ gradient followed by an isothermal step of 10 min at 280 °C. The obtained data was processed with the TurboMass Software and Bibliographic searches where performed with NIST MS Search 2.0.

Conventional Thermogravimetric Analysis coupled with Mass Spectrometry (TG-MS)

Netzsch STA 409CD Skimmer with an EI ion source and a quadrupole mass spectrometer. Time-dependent temperature profile: 25–700 °C (20 K min^{-1} temperature ramp) and cooling to 30 º C. The initial sample weights were adjusted at 5.0 (±0.1) mg and the whole experiment was executed under inert gas atmosphere with a He gas flow of 80 $mL\,min^{-1}$.

TEM:

A double Cs-corrected FEI Titan Themis 300 with excited monochromator has been used for imaging. The Cs corrector of the objective lens has been tuned to a negative Cs of -10 µm and images were recorded in slight underfocus (negative Cs imaging conditions). The excited monochromator reduces the energy spread of the illumination resulting of a beam energy spread of 180 meV to reduce the chromatic aberration. Images were recorded on a FEI CETA 4k CMOS camera with a dwell time of 1 s and, if necessary, an applied binning. TEM samples were prepared by drop casting a sonicated suspension of the sample in ethanol onto Cu grids coated with a holey carbon film layer.

Nitrogen adsorption isotherms:

The measurements were performed on a Quantachrome Quadrasorb SI porosimeter and a Micromeritics TriStar3000 instrument. The SSAs were determined according to the multipoint Brunauer-Emmett-Teller (BET) model using the data points suggested by the micropore BET assistant of the Quantachrome software (however, not exceeding the range of 0.05 - 0.30 $p \cdot p_0^{-1}$) or the Micromeritics software.

Electrochemical measurements:

The oxygen reduction reaction activity of the materials was investigated with a three-electrode rotating disk electrode (RDE) setup (Gamry Instruments) in 0.1 M KOH (Titripur®, Merck). As counter and reference electrode served a $Ag/AgCl_{sat}$-electrode and a graphite rod (diameter 6 mm), respectively. All given potentials were converted to the RHE scale and corrected to the internal resistance determined by impedance at high frequencies. Typically, 5 mg of the ball-milled catalyst were mixed with 50 µL of Nafion® solution (5 wt.% in lower aliphatic alcohols and water) and 95 µL of absolute ethanol (VWR) for catalyst ink preparation. The resulting mixture was sonicated for 30 min supporting a homogenous dispersion. Subsequently, an ink aliquot of 5 µL was drop-coated onto the well-polished glassy carbon electrode (Gamry Instruments; diameter, 5.0 mm) and dried at 50 °C under ambient conditions. The procedure resulted in a catalyst loading of 290 µg cm^{-2}. Prior to testing the electrodes were cycled for 10 cycles between 0.0 and 1.0 V (vs. RHE) in O_2-saturated solution to guarantee stable cyclic voltammograms (CVs). Linear sweep voltammograms (LSVs) and CVs were conducted with a sweep rate of 5 mVs^{-1} and 50 mvs^{-1},

respectively. The LSVs were corrected to the double layer capacity by subtracting the LSV obtained in nitrogen-saturated solution.

The LSVs obtained at different rotation rates were used for Koutecký-Levich (KL) analysis. KL diagrams for different potentials were received by plotting the reciprocal currents (i^{-1}) vs. the reciprocal square route of the angular rotating speeds ($\omega^{-1/2}$). The slopes of the linear fit lines can be used for the calculation of the electron transfer number (n) according to the KL equation (Equation 1).

$$\frac{1}{i} = \frac{1}{i_L} + \frac{1}{i_K} = \frac{1}{B\omega^{\frac{1}{2}}} + \frac{1}{i_K} \qquad (1)$$

with $B = 0.62nFAC_0D^{\frac{2}{3}}\nu^{-\frac{1}{6}}$

Here i_K and i_L represent the kinetic and the diffusion limiting current, respectively. F stands for the Faraday constant (96,485 $Cmol^{-1}$) and A is the area of the electrode (0.196 cm^2). C_0 is the saturated O_2 concentration ($1.21x10^{-6}$ $mol \cdot cm^{-3}$), D the diffusion coefficient of the dissolved O_2 ($1.86x10^{-5}$ $cm^2 \cdot s^{-1}$) and υ the kinematic viscosity of the electrolyte (0.01 $cm^2 \cdot s^{-1}$). All given values apply for 0.1 M KOH at room temperature.

2 Statistical Raman Spectroscopy of SWCNT-Ph and SWCNT-BiPh Synthesized Using THF as a Solvent

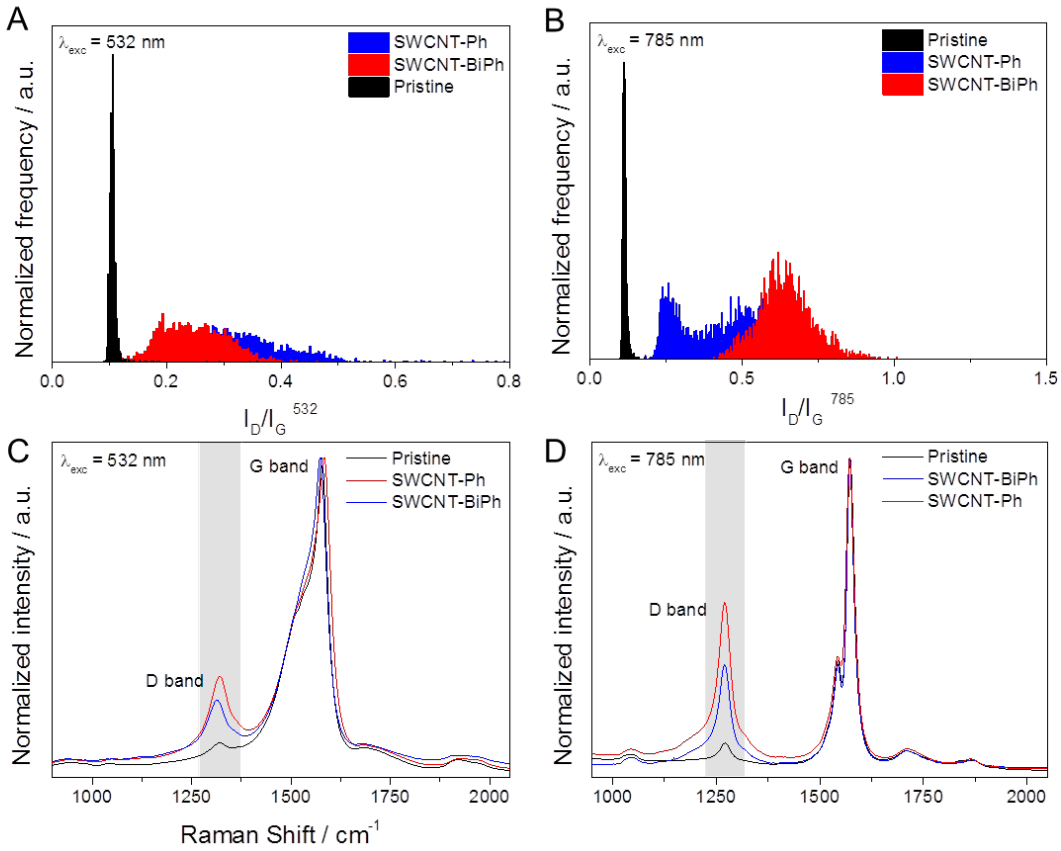

Figure S1: Statistical Raman spectroscopy of SWCNT-Ph, SWCNT-BiPh, and pristine HiPco SCWNTs samples synthesized using THF instead of DMAc (>600 single point spectra each). A) Statistical distribution of the I_D/I_G values at 532 nm and B) 785 nm laser excitation wavelengths. C) Mean spectra measured at 532 nm and D) 785 nm laser excitation wavelengths.

3 Statistical Raman Spectroscopy of SWCNT-Ph* and SWCNT-BiPh* Synthesized *via* Diazonium Route Without Using KC_4 Nanotubide Salts

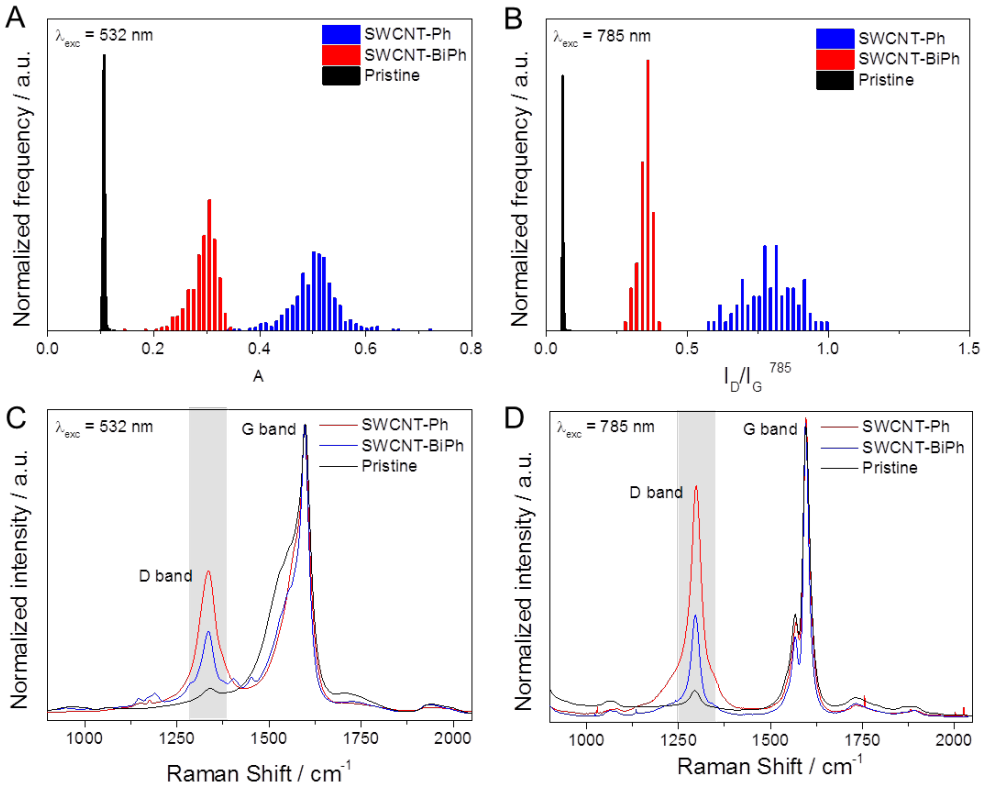

Figure S2: Statistical Raman spectroscopy of SWCNT-Ph*, SWCNT-BiPh*, and pristine HiPco SCWNTs samples synthesized without using KC_4 nanotubide salts. In these experiments CHP was employed as solvent for solubilizing the nanotubes (>600 single point spectra each). A) Statistical distribution of the I_D/I_G values at 532 nm and B) 785 nm laser excitation wavelengths. C) Mean spectra measured at 532 nm and D) 785 nm laser excitation wavelengths.

4 Statistical Raman Spectroscopy of SWCNT-Ph and SWCNT-BiPh Synthesized Using Elicarb Nanotubes

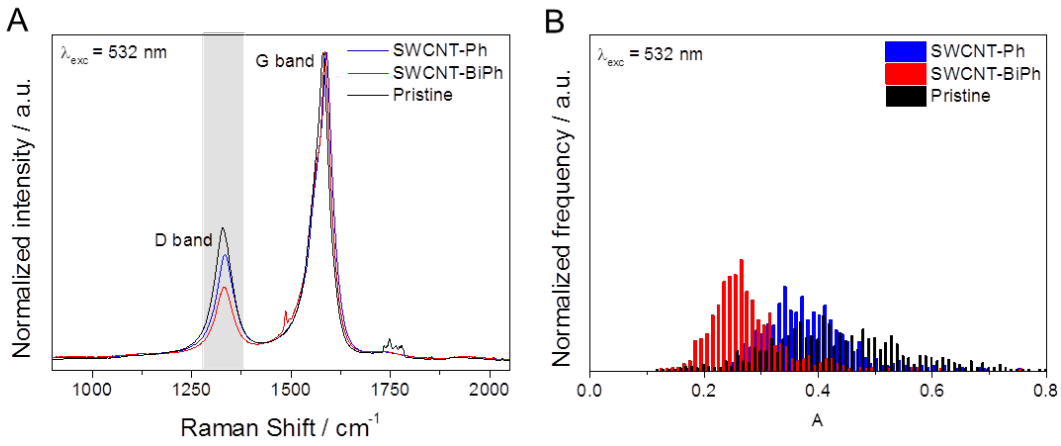

Figure S3: : Statistical Raman spectroscopy of SWCNT-Ph, SWCNT-BiPh, and pristine Elicarb SCWNTs samples (>600 single point spectra each). A) Statistical distribution of the I_D/I_G values at 532 nm and B) Mean spectra measured at 532 nm laser excitation wavelength.

5 Statistical Raman Spectroscopy of SWCNT-Naph Synthesized Using THF as a Solvent

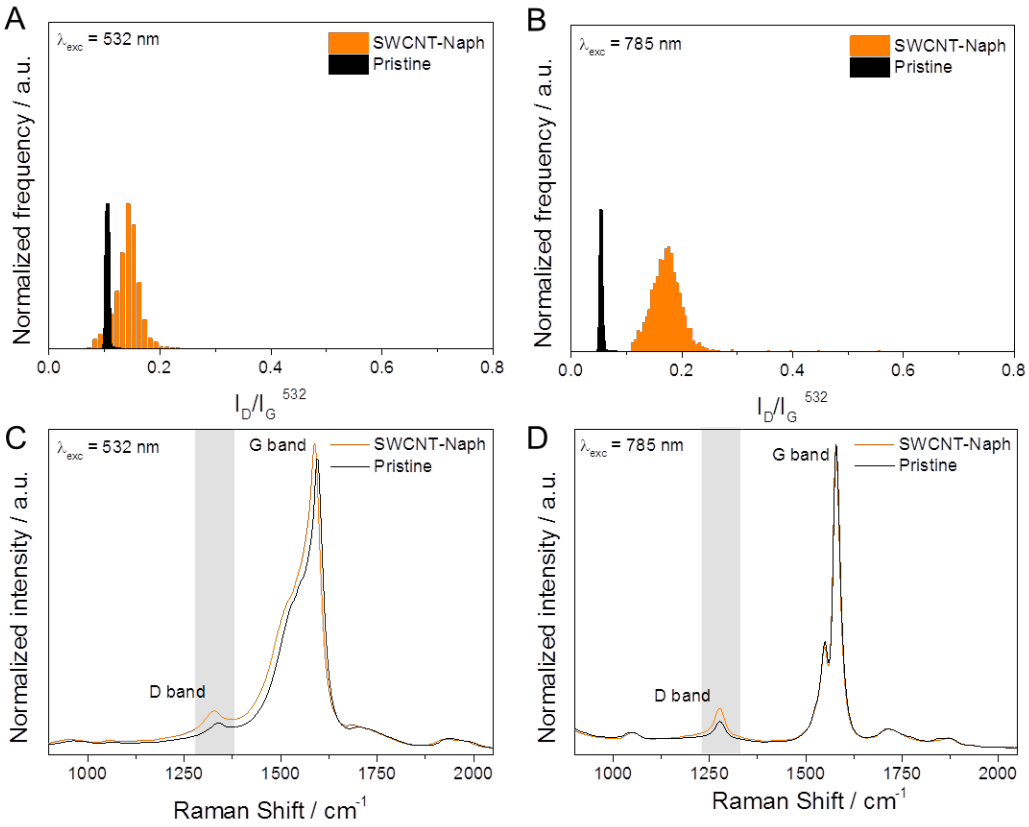

Figure S4: Statistical Raman spectroscopy of SWCNT-Naph and pristine HiPco SCWNTs samples synthesized using THF as a solvent (>600 single point spectra each). A) Statistical distribution of the I_D/I_G values at 532 nm and B) 785 nm laser excitation wavelengths. C) Mean spectra measured at 532 nm and D) 785 nm laser excitation wavelengths.

6 Additional Molecular Linkers Explored

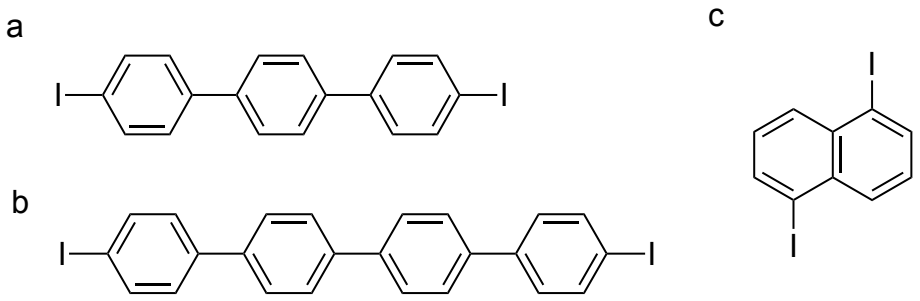

Figure S5: Chemical structures of additional molecular linkers used in the study. A) 4,4’’-diiodo-*p*-terphenyl, B) 4,4’’’-diiodo-*p*-quaterphenyl, and C) 1,5-*p*-diiodonaphtalene.

7 Additional TEM measurments

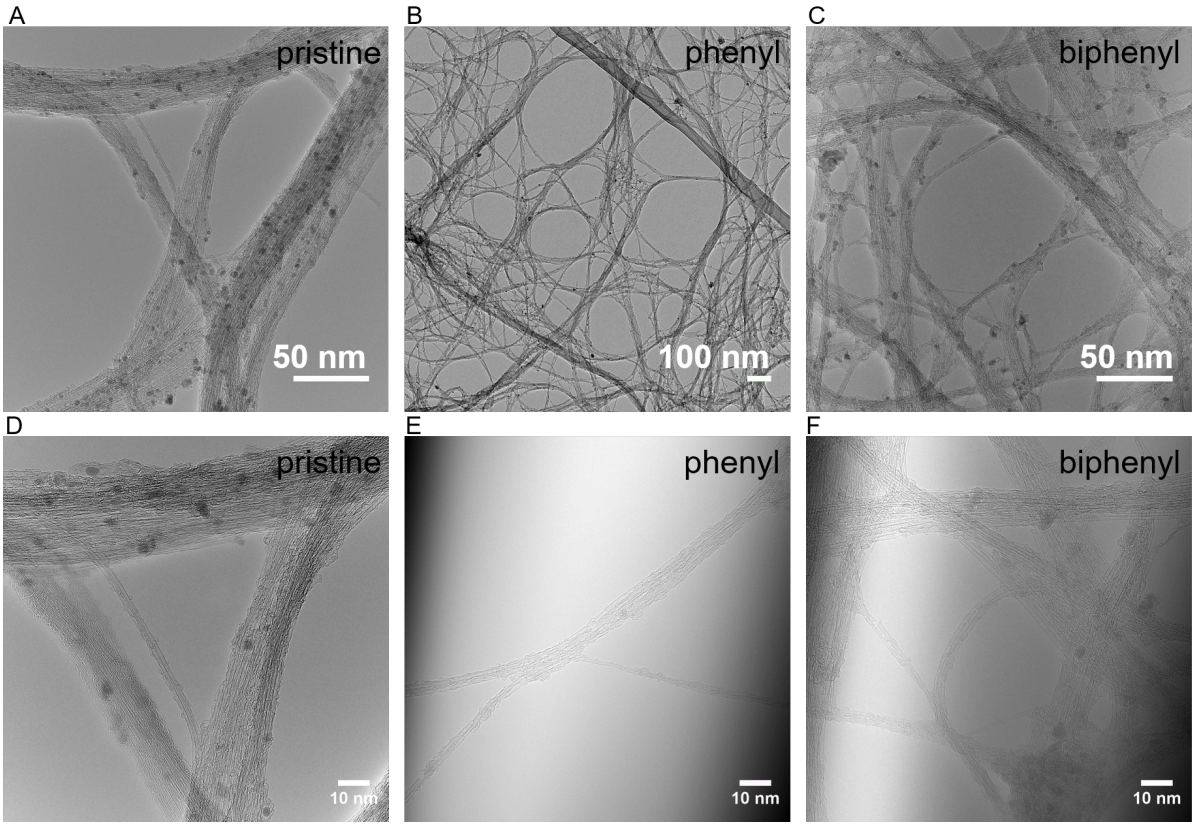

Figure S6: A-C) Overview BF-TEM images of pristine (A), phenyl-functionalized (B) and biphenyl-functionalized SWCNT (C). Mind the different scale bar in (B). D-F) HRTEM of pristine (D) and functionalized SWCNTs (E-F) as indicated.

8 Nitrogen-physisorption Measurements of the Pristine SWCNT

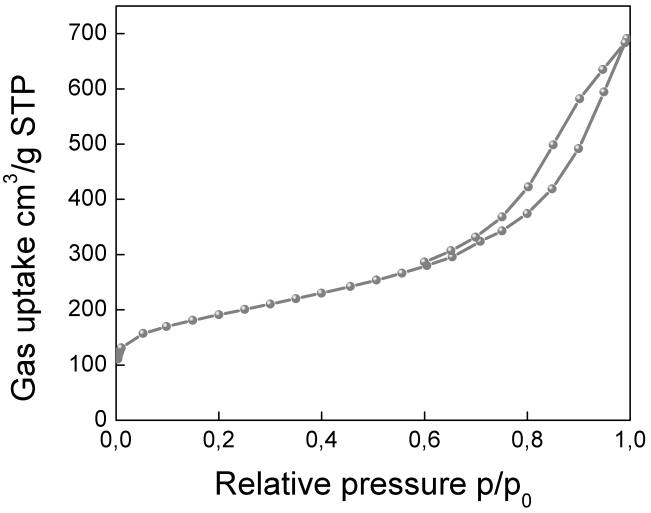

Figure S7: Nitrogen adsorption-desorption isotherm of the pristine SWCNT.

9 RDE polarization curve of the Pristine SWCNT

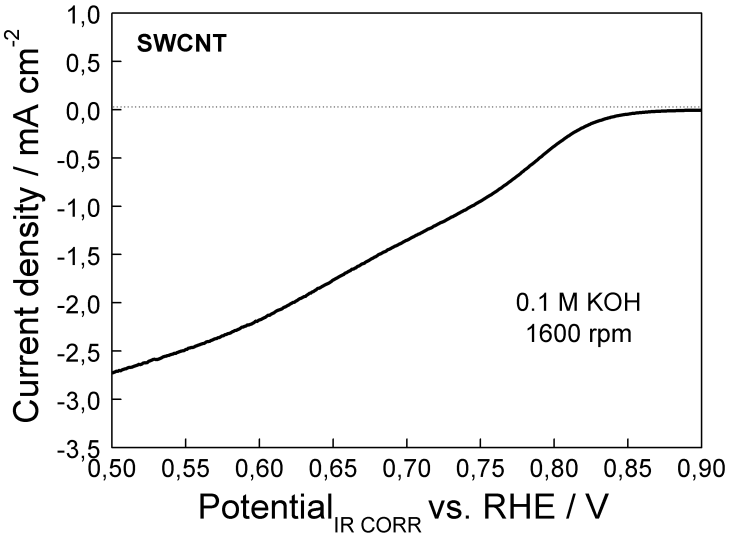

Figure S8: RDE polarization curves of pristine SWCNT in O_2-saturated 0.1 M KOH with a sweep rate of 5 mV s^{-1}, 1,600 rpm.

9 Koutecký-Levich Analysis

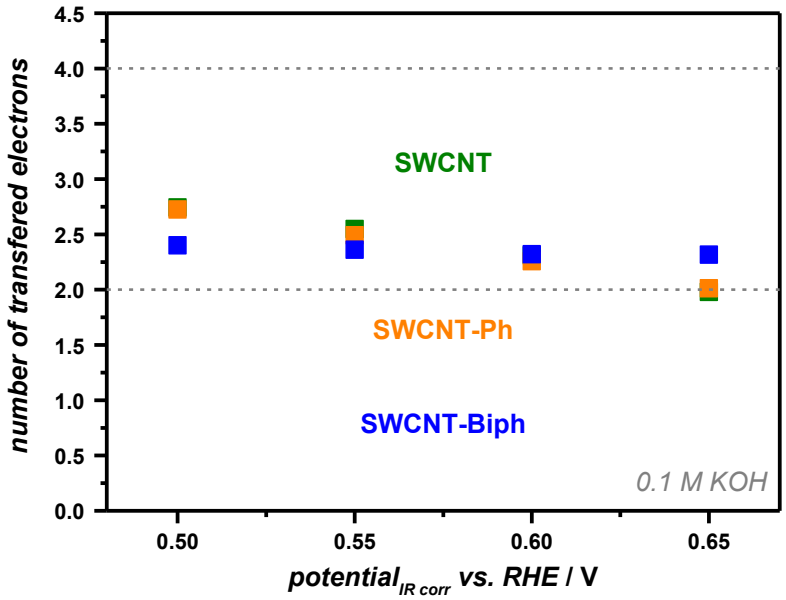

Figure S9: Koutecký-Levich analysis of the materials at different potentials obtained from polarization curves at different rotation rates.

10 Transmission Electron Microscopy Image Series

VIDEO-1: SM_BiPh on SWCNT: Image series of functional group (BiPh) on SWCNT. The group undergoes several conformational changes before it detaches at the end of the image series. Scale bar is 2 nm.

VIDEO-2: SM_vibration_SWCNT-BiPh: Image series showing correlated movement of SWCNT-Biph bundles. The correlated dynamic behaviour can be ascribed to an interconnectivity as a result of the covalent functionalization between the sidewalls of the tubes.

11 References

(1) Iwamoto, T.; Watanabe, Y.; Sakamoto, Y.; Suzuki, T.; Yamago, S. *J. Am. Chem. Soc.* **2011**, *133*, 8354.